新型单自由度六连杆机械压力机机构的静力学及动力学分析

陈修龙[1],高文花[1],姜　帅[1],宋　浩[1],苟岩岩[2]
(1.山东科技大学 机械电子工程学院,山东 青岛 266590; 2.泰山职业技术学院 机电工程系,山东 泰安 271000)

摘　要:提出了一种新型的单自由度六连杆机械压力机机构,为了实现机构的动态静力学以及动力学分析,采用复数矢量法建立了机构的运动学模型,基于达朗贝尔原理建立了机构的动态静力学方程,利用拉格朗日法建立了机构的动力学方程;分别利用 MATLAB 理论计算与 ADAMS 虚拟样机仿真得到压力机机构中滑块的位置曲线、速度曲线、加速度曲线,以及曲柄的平衡力矩和驱动力矩变化曲线。研究不仅为六连杆压力机运动学分析、平衡力矩和驱动力矩的求解和结构设计提供了理论依据,也为其他压力机机构的静力学和动力学分析提供了有效方法。

关键词:六连杆机构;运动学分析;静力学;动力学

中图分类号:TH112　　**文献标志码**:A　　**文章编号**:1672-3767(2017)05-0080-11

DOI:10.16452/j.cnki.sdkjzk.2017.05.012

Static and Dynamic Analysis of a Novel Single-DOF Six-bar Mechanical Press Mechanism

CHEN Xiulong[1], GAO Wenhua[1], JIANG Shuai[1], SONG Hao[1], GOU Yanyan[2]
(1. College of Mechanical and Electronic Engineering, Shandong University of Science and Technology, Qingdao, Shandong 266590, China; 2. Department of Mechanical and Electronic Engineering, Taishan Vocational and Technical College, Taian, Shandong 271000, China)

Abstract: In this paper, a novel single-DOF six-bar mechanical press mechanism is proposed. In order to realize the static and dynamic analysis of this six-bar mechanism, a kinematic model was established by complex number vector method. The kinetostatic equation and kinetic equation of the mechanism were established by D'Alembert Principle and Lagrange Method respectively. Finally, theoretical computation and simulation were carried out by using MATLAB and ADAMS virtual prototype respectively to obtain the curves ofthe position, velocity andacceleration of the slider, and the changing curves of the balance moment and driving torque of the articulate. The research can not only provide theoretical basis for kinematic analysis, the solution and physical design of balance moment and driving torque of the six-bar mechanism, but it can also provide an effective method for the static and kinematic analyses of other multi-link mechanisms.

Key words: six-bar mechanism; kinematic analysis; statics; dynamics

As a new type of forging equipment, multi-link mechanical press has the advantages of high working accuracy, good operation, excellent dynamic performance and high production efficiency[1-3]. Nowmulti-link mechanical press has been applied in many important fields[4-5], such as automotive, military, aerospace, etc.

收稿日期:2017-03-02
基金项目:国家自然科学基金项目(51005138);山东省优秀中青年科学家奖励基金项目(BS2012ZZ008)
作者简介:陈修龙(1976—),男,河北沧州人,副教授,博士,博士生导师,主要从事机构学理论和应用技术的研究.
E-mail:cxldy99@163.com

Static and dynamic analyses of multi-link mechanical press mechanism, which is the foundation of study on stiffness and control system design, can also provide an important theoretical basis for structure design of the mechanism. Up to now, domestic and overseas scholars have done a large number of researches on multi-link mechanism and achieved a series of research results in these areas[6-10]. Du et al. [11] designed a new type of hybrid driven seven bar press mechanism, which realized the journey and velocity control of the working table of the press. Guo et al.[12] studied on the trajectory planning and optimization of the variable velocity servo motor drive crank, using hybrid servo presses of feedback control, to achieve different stamping movement. Li et al. [13] put forward the idea of hybrid driven press, and introduced the characteristics of the hybrid drive machine, and the feasibility of the research of hybrid drive machine is prospected. Zhou et al. [14] studied the optimization of main driving mechanism for servo-punch press. However, there have been few efforts made oriented to analytical modeling which contains kinematic model, kinetostatics model and dynamic model at the same time. Then the static and dynamic analyses have not been sufficiently considered.

This paper takes a six-bar mechanism as an example, the analytical models of the mechanism are established, and kinematics and force analysis of the mechanism are carried out. Based on the kinematic analysis, the displacement, velocity and acceleration equations of the press are derived by using the complex vector method. Considering the gravity and inertia force of each component, the dynamic and statics analysis of the six-bar mechanical press is carried out. And the dynamic model of the press is established by using Lagrange method. Finally, by numerical computation and virtual prototype simulation, the correctness of the analytical models is verified. According to this, the structure model of the six-bar mechanical press is designed, as shown in Fig. 1.

1 Kinematics model of the six-bar mechanical press mechanism

1.1 Architectural feature of the six-bar mechanism

As shown in Fig. 1, this novel six-bar mechanism which is proposed in this paper includes Frame 1, Crank 2, Linkage 3, Quarter Panel 4, Linkage 5 and Slider 6. Crank 2 and Quarter Panel 4 are respectively connected with a machine frame through a revolute joint; Crank 2 is connected with servo motor and driven by the motor; Linkage 3 is connected with Crank 2 through a revolute joint; Linkage 3 and Linkage 5 are respectively connected with Quarter Panel 4 through a revolute joint; the end of Linkage 5 is connected with Slider 6 through a revolute joint; Slider 6 is in the fixed guide rail, which can move only in the vertical direction. The degree of freedom of the mechanism is one, and the motion of the mechanism can be driven by Crank 2. The structure chart of six-link mechanical press is shown in Fig. 2.

1.2 Displacement model of the mechanism

As shown in Fig. 1, the length of Crank 2 of the six-bar mechanism is expressed as L_2, the vector of Crank 2 is expressed as $\vec{\boldsymbol{L}}_2$, the vector angle, which is measured between the vector of the rod and the positive direction of the x axis along the counter clockwise direction, is expressed as θ_2. The rest members of the mechanical press mechanism can be expressed as the corresponding bar vector, and finally a closed vector polygon consisting of bar vectors is formed. Then the position model of the mechanical press mechanism is given by

$$\begin{cases} \vec{\boldsymbol{L}}_2+\vec{\boldsymbol{L}}_3=\vec{\boldsymbol{L}}_1+\vec{\boldsymbol{L}}_{41} \\ \vec{\boldsymbol{L}}_{42}+\vec{\boldsymbol{L}}_5+\vec{\boldsymbol{L}}=\vec{\boldsymbol{S}}_6 \end{cases}. \tag{1}$$

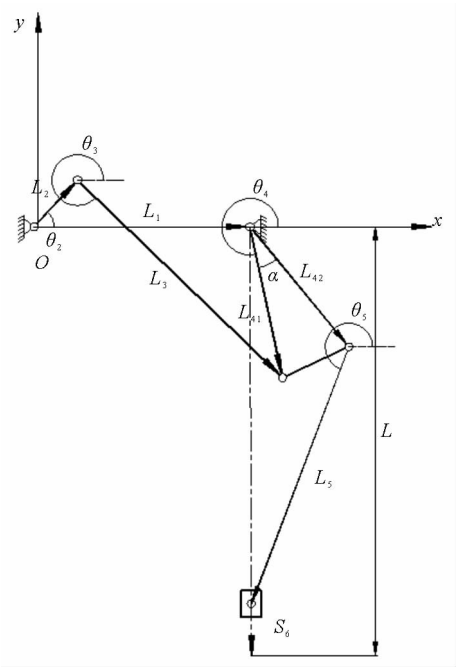

Fig. 1 Structure diagram of six bar mechanism

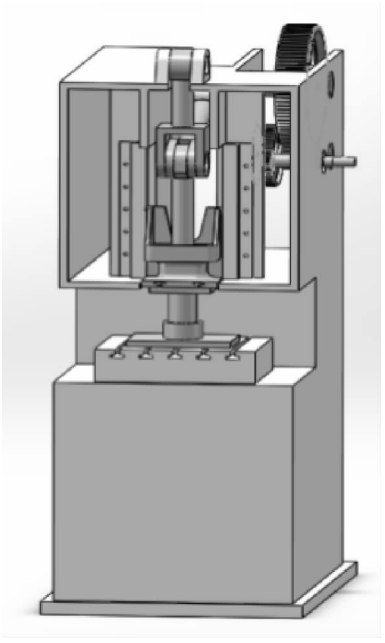

Fig. 2 Structure chart of six-link mechanical press

From Formula(1), we can obtain

$$\begin{cases} L_2\cos\theta_2+L_3\cos\theta_3=L_1\cos\theta_1+L_{41}\cos\theta_4 \\ L_2\sin\theta_2+L_3\sin\theta_3=L_1\sin\theta_1+L_{41}\sin\theta_4 \\ L_{42}\cos(\theta_4+\alpha)+L_5\cos\theta_5=0 \\ L_{42}\sin(\theta_4+\alpha)+L_5\sin\theta_5-S_6=-L \end{cases}. \tag{2}$$

In the Formula(2), the motion law of Crank 2 and the length of each member are known. Therefore, three unknown direction angles θ_3, θ_4, θ_5 and the displacement of the slider S_6 are given by

$$\begin{cases} \theta_4=2\arctan\dfrac{A-\sqrt{A^2+B^2-C^2}}{B-C} \\ \theta_3=-\arccos\left(\dfrac{L_1\cos\theta_1+L_{41}\cos\theta_4-L_2\cos\theta_2}{L_3}\right) \\ \theta_5=\arccos\left(\dfrac{-L_{42}\cos(\theta_4+\alpha)}{L_5}\right) \\ S_6=L+L_{42}\sin(\theta_4+\alpha)+L_5\sin\theta_5 \end{cases}. \tag{3}$$

Where, L_1, L_2, L_3, L_{41}, L_{42}, L_5, L, S_6, α are the dimension parameters of the mechanism as shown in Fig. 1.

$$A=-2L_2L_{41}\sin\theta_2, B=2L_1L_{41}-2L_2L_{41}\cos\theta_2, C=L_1^2+L_2^2+L_{41}^2-L_3^2-2L_1L_2\cos\theta_2.$$

1.3 Velocity model of the mechanism

Taking first derivative of Formula(2) with respect to time, we can get

$$\begin{cases}\omega_3=\dfrac{L_2\omega_2\sin(\theta_4-\theta_2)}{L_3\sin(\theta_3-\theta_4)}\\ \omega_4=\dfrac{L_2\omega_2\sin(\theta_3-\theta_2)}{L_{41}\sin(\theta_3-\theta_4)}\\ \omega_5=\dfrac{L_{42}\omega_4\sin(\theta_4+\alpha)}{-L_5\sin\theta_5}\\ V_6=L_{42}\omega_4\cos(\theta_4+\alpha)+L_5\omega_5\cos\theta_5\end{cases}. \tag{4}$$

Where, ω_i is the angular velocity of the link i, V_6 is the velocity of Slider 6.

1.4 Acceleration model of the mechanism

Taking the second derivative of equation (2) with respect to time, the acceleration of the six-bar mechanism can be expressed as

$$\begin{cases}\alpha_3=\dfrac{-L_2\omega_2^2\cos(\theta_2-\theta_4)-L_3\omega_3^2\cos(\theta_3-\theta_4)+L_{41}\omega_4^2}{L_3\sin(\theta_3-\theta_4)}\\ \alpha_4=\dfrac{L_2\omega_2^2\cos\theta_2+L_3\omega_3^2\cos\theta_3+L_3\alpha_3\sin\theta_3-L_{41}\omega_4^2\cos\theta_4}{L_{41}\sin\theta_4}\\ \alpha_5=\dfrac{L_{42}\omega_4^2\cos(\theta_4+\alpha)+L_{42}\alpha_4\sin(\theta_4+\alpha)+L_5\omega_5^2\cos\theta_5}{-L_5\sin\theta_5}\\ a_6=-L_{42}\omega_4^2\sin(\theta_4+\alpha)+L_{42}\alpha_4\cos(\theta_4+\alpha)-L_5\omega_5^2\sin\theta_5+L_5\alpha_5\cos\theta_5\end{cases}. \tag{5}$$

Where, α_i is the angular acceleration velocity of the link i, a_6 is the acceleration of Slider 6.

2 Kinetostatics model of the six-bar mechanical press mechanism

2.1 Kinetostatics modeling of the mechanism

Kinetostatics analysis diagram of six-bar mechanism is shown in Fig. 3. From Fig. 3, the geometric parameters of components, such as the distance from the center of mass of the link to the front hinge, are expressed as L_{s2}, L_{s3}, L_{s4}, L_{s5}; the physical parameters, such as mass of component i and moment of inertia around its center of mass of component i, are expressed as m_i and J_i, respectively, where $i=2,3,4,5,6$. And x_{si}, y_{si} represent the x and y coordinates components of its center of mass of link i; $\dot{x}_{si}$, $\dot{y}_{si}$ represent the x and y velocity components of the center of mass of link$i$; $\ddot{x}_{si}$, $\ddot{y}_{si}$ represent the x and y acceleration components of the center of mass of link$i$; M_2 represents the balance moment of Crank 2; $F_{x_1x_2x}$, $F_{x_1x_2y}$ represent the force of x_2 to x_1 in x direction and in y direction; F_{x_1x}, F_{x_1y} represent the force of frame to x_1 in x direction and in y direction.

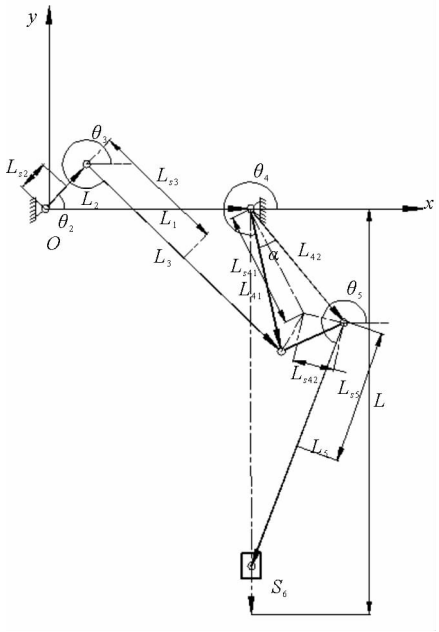

Fig. 3 Schematic diagram of single DOF six-bar mechanism

The force analysis of Crank 2, Link 3, Link 4, Link 5 and Slider 6 are shown in Fig. 4, Fig. 5, Fig. 6, Fig. 7, Fig. 8 respectively.

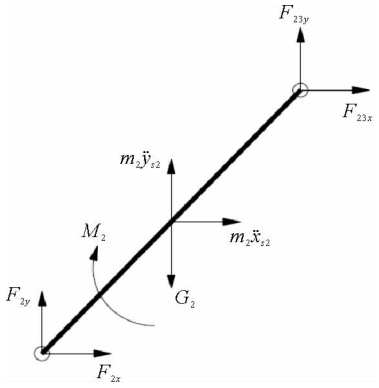

Fig. 4 Force analysis of crank

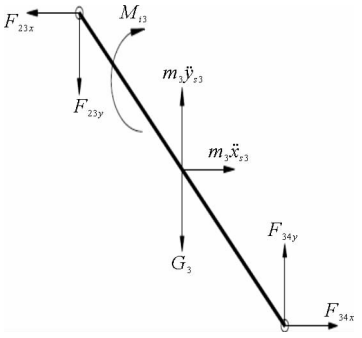

Fig. 5 Force analysis of Link 3

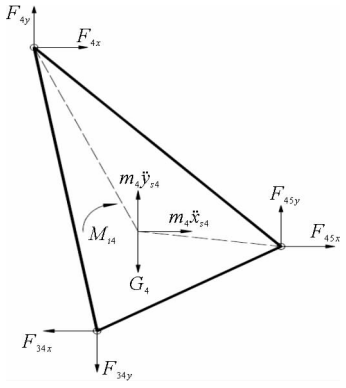

Fig. 6 Force analysis of quarter panel

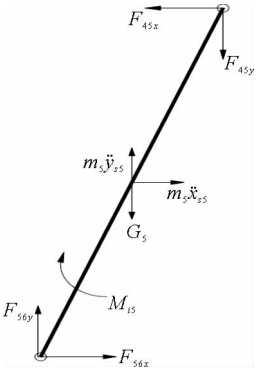

Fig. 7 Force analysis of linkage

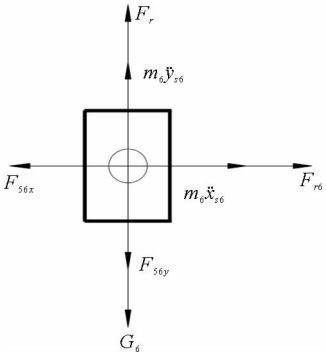

Fig. 8 Force analysis of slider

Through the analysis of the above five components, we can make a list of the fourteen balance equations. Because the Fourteen equations are linear equations, it can be sorted into the following matrix in accordance with the order of unknown forces on the members 2, 3, 4, 5, 6, and so on. Then we can get

$$\boldsymbol{CF}=\boldsymbol{D} \quad . \tag{6}$$

Where $\boldsymbol{F}=[M_2 \quad F_{2x} \quad F_{2y} \quad F_{23x} \quad F_{23y} \quad F_{34x} \quad F_{34y} \quad F_{45x} \quad F_{45y} \quad F_{4x} \quad F_{4y} \quad F_{56x} \quad F_{56y} \quad F_{r6}]_{14\times1}$ is an unknown force array,

$\boldsymbol{D}=[-m_2\ddot{x}_{s2} \quad G_2-m_2\ddot{y}_{s2} \quad 0 \quad -m_3\ddot{x}_{s3} \quad G_3-m_3\ddot{y}_{s3} \quad J_3\alpha_3 \quad -m_4\ddot{x}_{s4} \quad G_4-m_4\ddot{y}_{s4}-m_4\ddot{x}_{s4}L_{s4}\sin(2\pi-\theta_4-\alpha+\beta)-m_4\ddot{y}_{s4}L_{s4}\cos(2\pi-\theta_4-\alpha+\beta)+G_4L_{s4}\cos(2\pi-\theta_4-\alpha+\beta)+J_4\alpha_4 \quad -m_5\ddot{x}_{s5} \quad G_5-m_5\ddot{y}_{s5} \quad J_5\alpha_5 \quad -m_6\ddot{x}_{s6}-F_{r6} \quad G_6-m_6\ddot{y}_{s6}-F_r]_{14\times1}$ is known force array.

$$\ddot{x}_{s2}=-L_{s2}\omega_2^2\cos\theta_2-L_{s2}\alpha_2\sin\theta_2,\ddot{y}_{s2}=-L_{s2}\omega_2^2\sin\theta_2+L_{s2}\alpha_2\cos\theta_2,$$

$$\ddot{x}_{s3}=-L_2\omega_2^2\cos\theta_2-L_2\alpha_2\sin\theta_2-L_{s3}\omega_3^2\cos\theta_3-L_{s3}\alpha_3\sin\theta_3,$$

$$\ddot{y}_{s3}=-L_2\omega_2^2\sin\theta_2+L_2\alpha_2\cos\theta_2-L_{s3}\omega_3^2\sin\theta_3+L_{s3}\alpha_3\cos\theta_3,$$

$$\ddot{x}_{s4}=-L_{s4}\omega_4^2\cos(\theta_4+\alpha-\beta)-L_{s4}\alpha_4\sin(\theta_4+\alpha-\beta),$$

$$\ddot{y}_{s4}=-L_{s4}\omega_4^2\sin(\theta_4+\alpha-\beta)+L_{s4}\alpha_4\cos(\theta_4+\alpha-\beta),$$

$$\ddot{x}_{s5}=-L_{42}\omega_4^2\cos(\theta_4+\alpha)-L_{42}\alpha_4\sin(\theta_4+\alpha)-L_{s5}\omega_5^2\cos\theta_5-L_{s5}\alpha_5\sin\theta_5,$$

$$\ddot{y}_{s5}=-L_{42}\omega_4^2\sin(\theta_4+\alpha)+L_{42}\alpha_4\cos(\theta_4+\alpha)-L_{s5}\omega_5^2\sin\theta_5+L_{s5}\alpha_5\cos\theta_5,$$

$$\ddot{x}_{s6}=0,\ddot{y}_{s6}=-L_{42}\omega_4^2\sin(\theta_4+\alpha)+L_{42}\alpha_4\cos(\theta_4+\alpha)-L_5\omega_5^2\sin\theta_5+L_5\alpha_5\cos\theta_5,$$

$$\boldsymbol{C}=\begin{bmatrix}
0 & 1 & 0 & 1 & 0 & 0 & 0 & 0&0&0&0&0&0&0\\
0 & 0 & 1 & 0 & 1 & 0 & 0 & 0&0&0&0&0&0&0\\
1 & L_{s2}\sin\theta_2 & -L_{s2}\cos\theta_2 & (L_{s2}-L_2)\sin\theta_2 & (L_2-L_{s2})\cos\theta_2 & 0 & 0 & 0&0&0&0&0&0&0\\
0 & 0 & 0 & -1 & 0 & 1 & 0 & 0&0&0&0&0&0&0\\
0 & 0 & 0 & 0 & -1 & 0 & 1 & 0&0&0&0&0&0&0\\
0 & 0 & 0 & -L_{s3}\sin\theta_3 & L_{s3}\cos\theta_3 & (L_{s3}-L_3)\sin\theta_3 & (L_3-L_{s3})\cos\theta_3 & 0&0&0&0&0&0&0\\
0 & 0 & 0 & 0 & 0 & -1 & 0 & 1&0&1&0&0&0&0\\
0 & 0 & 0 & 0 & 0 & -1 & 0 & 1&0&1&0&0&0&0\\
0 & 0 & 0 & 0 & L_{41}\sin\theta_4 & -L_{41}\cos\theta_4 & -L_{42}\sin(\theta_4+\alpha) & L_{42}\cos(\theta_4+\alpha) & 0&0&0&0&0&0\\
0 & 0 & 0 & 0 & 0 & 0 & -1 & 0&0&0&1&0&0&0\\
0 & 0 & 0 & 0 & 0 & 0 & 0 & -1&0&0&0&1&0&0\\
0 & 0 & 0 & 0 & 0 & 0 & -L_{s5}\sin\theta_5 & L_{s5}\cos\theta_5 & 0&0&(L_{s5}-L_5)\sin\theta_5&(L_5-L_{s5})\cos\theta_5&0&0\\
0 & 0 & 0 & 0 & 0 & 0 & 0 & 0&0&-1&0&1&0&0\\
0 & 0 & 0 & 0 & 0 & 0 & 0 & 0&0&0&0&-1&0&0
\end{bmatrix}_{14\times14}$$

is an unknown force coefficient matrix.

3 Dynamics model of the six-bar mechanical press mechanism

3.1 Generalized coordinates of the mechanism

From Fig. 2, Crank 2 is the driving link in the single degree of freedom six-bar mechanism. When the angular displacement of Crank 2 is given, the position of the whole mechanism is also determined, and thus, the angular displacement of the crank can be taken as the generalized coordinates, that is $q=\theta_2$.

The Lagrange formula for a single degree of freedom system is expressed as

$$\frac{\mathrm{d}}{\mathrm{d}t}\left(\frac{\partial \mathrm{E}}{\partial \dot{q}}\right)-\frac{\partial E}{\partial q}+\frac{\partial V}{\partial q}=Q \quad . \tag{7}$$

Where, E, V, Q, q are the kinetic energy, potential energy, generalized force and generalized coordinates of the system, respectively.

3.2 The Lagrange dynamic equation of the mechanism

3.2.1 Motion analysis of the mechanism

To calculate the kinetic energy of the mechanism, we must know the angular velocity and the velocity of the center of mass of each member. By kinematic analysis of the mechanism, we can get

$$\begin{cases}\theta_i=\theta_i(q)\\ x_{si}=x_{si}(q)\\ y_{si}=y_{si}(q)\end{cases} \quad . \tag{8}$$

Where θ_i is the angular displacement of component i, x_{Si} and y_{Si} are the coordinates of the centroid of the component in the x axis and y axis.

Taking derivative of equation (8) with respect to time, the angular velocity $\dot{\theta}_i$ of the component i, the speed of centroid $\dot{x}_{Si}$ in the x axis and $\dot{y}_{Si}$ in the y axis can be obtained as

$$\dot{\theta}_i=\frac{\partial \theta_i}{\partial q}\dot{q} \quad , \tag{9}$$

$$\begin{cases}\dot{x}_{si}=\dfrac{\partial x_{si}}{\partial q}\dot{q}\\ \dot{y}_{si}=\dfrac{\partial y_{si}}{\partial q}\dot{q}\end{cases} \quad . \tag{10}$$

The velocity of the center of mass S_i can be given by

$$v_{si}=\sqrt{\dot{x}_{si}^2+\dot{y}_{si}^2} \quad . \tag{11}$$

3.2.2 Kinetic energy of the mechanism

The kinetic energy can be expressed as

$$E=\sum_{i=2}^{6}\frac{1}{2}(m_i v_{si}^2+J_i\dot{\theta}_i^2) \quad . \tag{12}$$

By substituting equation (9) and (11) into equation (12), the kinetic energy of the system can be given by

$$E=\frac{1}{2}J_e\dot{q}^2 \quad , \tag{13}$$

Where $J_e=\sum_{i=2}^{6}\left\{m_i\left[\left(\frac{\partial x_{si}}{\partial q}\right)^2+\left(\frac{\partial y_{si}}{\partial q}\right)^2\right]+J_i\left(\frac{\partial\theta_i}{\partial q}\right)^2\right\}$.

3.2.3 Potential energy of the mechanism

The zero potential energy position is located at the origin of the coordinate (see Fig. 3), the positive direction of the Y axis is the direction of gravity, the potential energy of the system is written as

$$V=m_2gy_{s2}+m_3gy_{s3}+m_4gy_{s4}+m_5gy_{s5}+m_6gy_{s6} \quad . \tag{14}$$

3.2.4 Generalized force of the mechanism

The generalized force can be determined according to the virtual work principle. For a single degree of freedom six-bar mechanism, the relationship between the virtual work δW of active force and the generalized virtual displacement can be given by

$$\delta W=Q\delta q \quad . \tag{15}$$

Where, the coefficient Q in front of generalized virtual displacement is generalized force.

For the single degree of freedom six-bar mechanism, according to the virtual work principle, we can get

$$\delta W=Q\delta q=M_2\delta q-F_r\left[\frac{\partial(L-S_6)}{\partial q}\delta q\right] \quad . \tag{16}$$

From the equation (16), the generalized force of the system is given by

$$Q=M_2+F_r\frac{\partial S_6}{\partial q} \quad . \tag{17}$$

Where, M_2 is the torque of the motor acting on the crank, S_6 is the displacement of the slider.

3.2.5 Motion differential equation of the mechanism

Taking derivative of equation (13) with respect to q and $\dot{q}$ respectively, we can get

$$\frac{\partial E}{\partial q}=\frac{1}{2}\dot{q}^2\frac{\partial J_e}{\partial q} \quad , \tag{18}$$

$$\frac{\mathrm{d}}{\mathrm{d}t}\left(\frac{\partial E}{\partial\dot{q}}\right)=\frac{\mathrm{d}(J_e\dot{q})}{\mathrm{d}t}=J_e\ddot{q}+\frac{\partial J_e}{\partial q}\dot{q}^2 \quad . \tag{19}$$

According to the equation(14) we can get

$$\frac{\partial V}{\partial q}=m_2g\frac{\partial y_{s1}}{\partial q}-m_3g\frac{\partial y_{s3}}{\partial q}-m_4g\frac{\partial y_{s4}}{\partial q}-m_5g\frac{\partial y_{s5}}{\partial q}-m_6g\frac{\partial y_{s6}}{\partial q} \quad . \tag{20}$$

Take formula(17), (18), (19) and (20) into Lagrange equation (7) and simplify it, the dynamic equation of the novel six-bar mechanism is expressed as

$$Q=J_e\ddot{q}+\frac{1}{2}\frac{\partial J_e}{\partial q}\dot{q}^2+\frac{\partial V}{\partial q} \quad . \tag{21}$$

4 Example of kinematic and force analysis of the six-bar mechanical press mechanism

4.1 System parameters of the mechanism

System parameters of the six-bar mechanism are shown in Tab. 1.

Tab. 1 System parameters of the six-bar mechanism

Designed parameter	Parameter values	Designed parameter	Parameter values
Distance between frameL_1/mm	430	Quality of Crank 2 m_2/kg	0.660
Distance from frames to bottom dead center of Sliding Block 6L/mm	650	Rotational speed of Crank 2 ω_2/(°/s)	120
Length of Crank 2 L_2/mm	90	Quality of Linkage 3 m_3/kg	2.998
Length of Linkage 3L_3/mm	464.7	Quality of Rocking-bar 4 m_4/kg	4.451
Length of QuarterPanel4 L_{41}/mm	250	Quality of Linkage 5 m_5/kg	2.594
Length of QuarterPanel4 L_{42}/mm	250	Quality of Sliding Block 6 m_6/kg	0.651
Length of Linkage 5 L_5/mm	400	Rotational inertia of Linkage 3 J_{3c}/(kg/m^2)	5.84×10^{-2}
Inclination angle of the frame θ_1/(°)	0	Rotational inertia of Rocking-bar 4 J_{4c}/(kg/m^2)	2.29×10^{-2}
Initial angle of Crank 2 θ_2/(°)	144.64	Rotational inertia of Linkage 5 J_{5c}/(kg/m^2)	3.80×10^{-2}

4.2 Example of kinematic analysis

When Crank 2 of the six-bar mechanism runs three cycles, the displacement curve of Slider 6 obtained by the numerical calculation of MATLAB and the displacement curve of Slider 9 obtained by the virtual proto type of ADAMS are shown in Fig. 9. The velocity curve of Slider 6 obtained by the numerical calculation of MATLAB and the velocity curve of Slider 6 obtained by the virtual prototype of ADAMS are shown in Fig. 10. The acceleration curve of Slider 6 obtained by the numerical calculation of MATLAB and the acceleration curve of Slider 6 obtained by the virtual prototype of ADAMS are shown in Fig. 11.

From Fig. 9 to Fig. 11, the trend and the peak value of the displacement curves, velocity curves, and acceleration curves are basically similar; the maximum error of the displacement, which occurs in 1.58 s, is 0.000 4 m; the maximum error of the velocity, which occurs in 1.98 s, is 0.000 3 m/s; the maximum error of the acceleration, which occurs in 1.64 s, is 0.000 5 m/s^2.

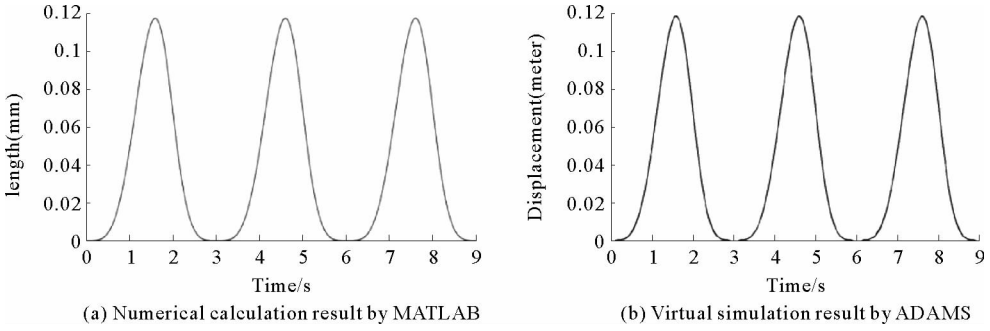

Fig. 9 The displacement of six-bar mechanism's slider

4.3 Example of kinetostatics analysis

When Slider 6 of the six-bar mechanism moves with no-load, that is $F_r=0$, the balance moment curves of crank of mechanism obtained by the numerical calculation of MATLAB and the balance moment

curves of crank of mechanism obtained by the virtual prototype of ADAMS are shown in Fig. 12. When Slider 6 of the six-bar mechanism moves with load, that is F_r=100 kN, the balance moment curves of crank of mechanism obtained by the numerical calculation of MATLAB and the balance moment curves of crank of mechanism obtained by the virtual prototype of ADAMS are shown in Fig. 13. The numerical calculation of the bearing reaction between Linkage 5 and Slider 6 and the virtual prototype simulation of the constraint force between Linkage 5 and Slider 6 are shown in Fig. 14.

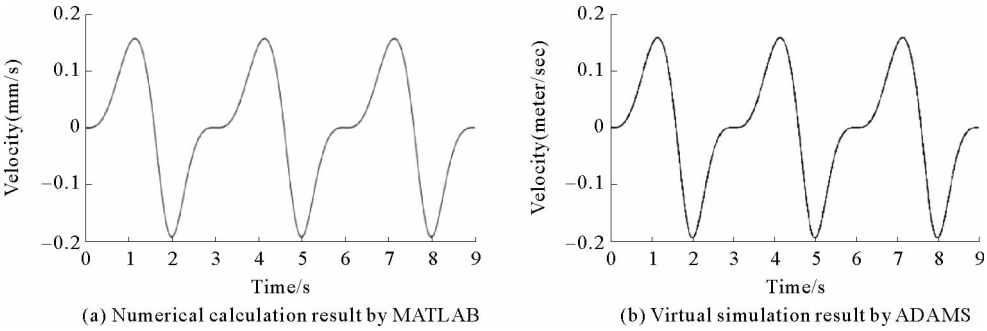

(a) Numerical calculation result by MATLAB (b) Virtual simulation result by ADAMS

Fig. 10 The velocity of six-bar mechanism's slider

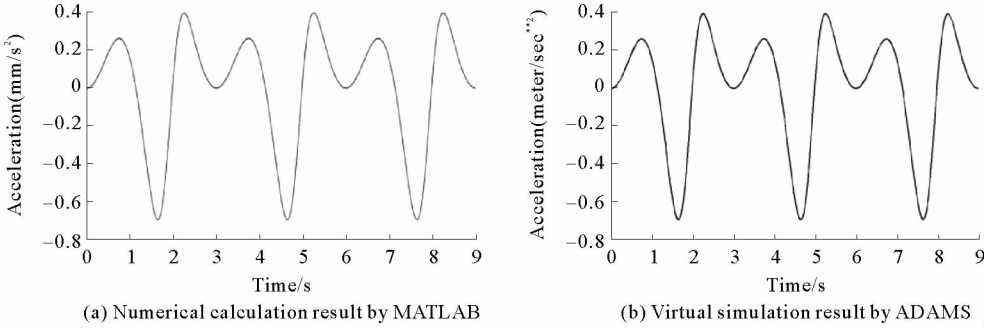

(a) Numerical calculation result by MATLAB (b) Virtual simulation result by ADAMS

Fig. 11 The acceleration of six-bar mechanism's slider

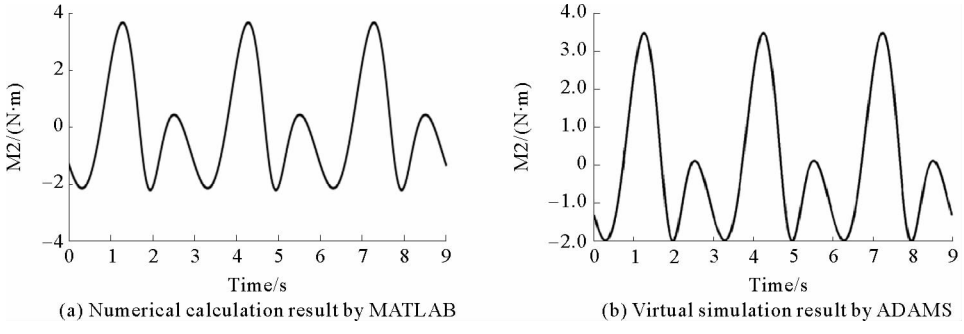

(a) Numerical calculation result by MATLAB (b) Virtual simulation result by ADAMS

Fig. 12 The balance moment of the six-bar mechanism when the slider has no load

From Fig. 12 to Fig. 14, the trend of MATLAB calculation result is consistent with the ADAMS virtual simulation result; when Slider 6 of the six-bar mechanism runs with no-load, the maximum error of the balance moment, which occurs in 1.28 s, is 0.198 2 N·m; when Slider 6 of the six-bar mechanism runs with load, the maximum error of the balance moment, which occurs in 1.98 s, is 14.332 4 N·m; when

Slider 6 of the six-bar mechanism runs with load, the maximum error of the constraint force between Linkage 5 and Slider 6, which occurs in 1.58 s, is 30 N.

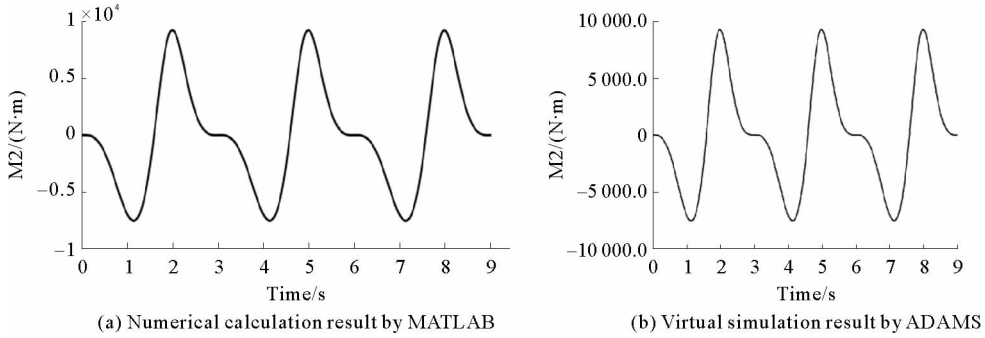

(a) Numerical calculation result by MATLAB (b) Virtual simulation result by ADAMS

Fig. 13 The balance moment of the six-bar mechanism when the slider has load

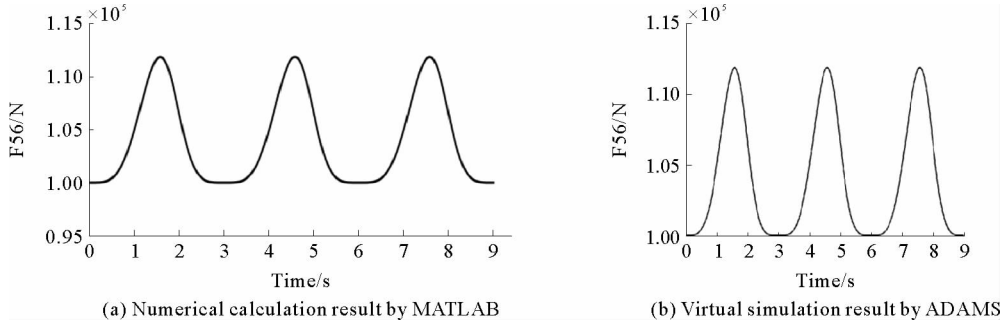

(a) Numerical calculation result by MATLAB (b) Virtual simulation result by ADAMS

Fig. 14 The constraint force between Linkage 5 and Slider 6 when the slider has load

4.4 Example of dynamics analysis

When Slider 6 of the six-bar mechanism moves with no-load, that is $F_r=0$, the numerical calculation of the driving torque of the crank obtained by MATLAB and the virtual prototype simulation of the driving torque of the crank obtained by ADAMS are shown in Fig. 15. When Slider 6 of the six-bar mechanism runs with load, that is $F_r=100$ kN, The numerical calculation of the driving torque of the crank obtained by MATLAB and the virtual prototype simulation of the driving torque of the crank obtained by ADAMS are shown in Fig. 16.

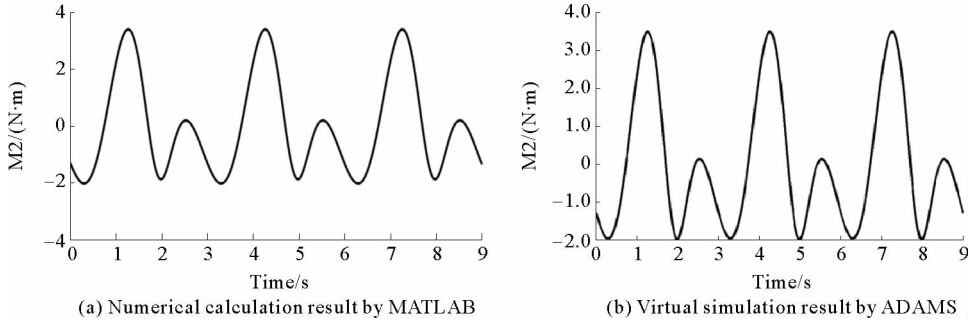

(a) Numerical calculation result by MATLAB (b) Virtual simulation result by ADAMS

Fig. 15 The driving torque of the six-bar mechanism when the slider has no load

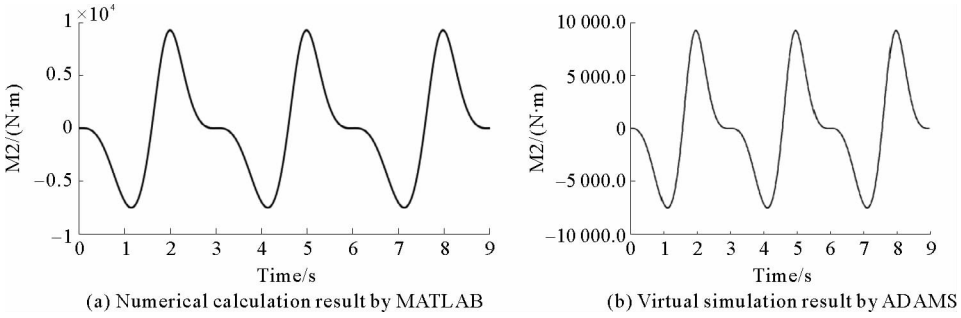

(a) Numerical calculation result by MATLAB (b) Virtual simulation result by ADAMS

Fig. 16 The driving torque of the six-bar mechanism when the slider has load

From Fig. 15 to Fig. 16, the trend of numerical calculation result is consistent with the virtual simulation result. When Slider 6 of the six-bar mechanism runs with no-load, the maximum error of the driving torque, which occurs in 1.26 s, is 0.058 8 N·m. When the slider 6 of six-bar mechanism runs with load, the maximum error of the driving torque, which occurs in 1.98 s, is 10.332 4 N·m.

5 Conclusions

1) A novel single-DOF six bar mechanical press mechanism is proposed. The kinematic model of this novel six-bar mechanism is established by using the complex vector method; the kinematic analysis including slider position, slider velocity, and slider acceleration is realized and verified by numerical calculation and virtual simulation.

2) The kinetostatics model of the six-bar mechanism is established by using the matrix method, the constraint force of joints and balance moment are studied and verified.

3) The dynamic model of the six-bar mechanism is established by using the Lagrange Method. The driving torque on crank is solved and verified.

4) This study can not only provide theoretical basis for kinematic analysis, force analysis and structure design of the six-bar mechanism, but also suggest a way of static and dynamic analysis for other multi-link mechanisms.

References

[1]TSO P L, LIANG K C. A nine-bar linkage for mechanical forming presses[J]. International Journal of Machine Tools & Manufacture, 2002, 42(1): 139-145.

[2]LIN W Q, LI Z S, LI J P, et al. Optimization method for movement of multi-bar press based on genetic algorithm[J]. Forging & Stamping Technology, 2011, 36(5): 81-84.

[3]GE Z H, MA W J, ZHANG K K, et al. Mechanism design and dynamic analysis of hybrid cam-linkage mechanical press[J]. Key Engineering Materials, 2011, 474-476: 803-806.

[4]SONG Q, LI J, YIN W. Mechanical press six-link mechanism design based on multi-objective[J]. Transactions of the Chinese Society for Agricultural Machinery, 2012, 43(4): 225-234.

[5]GAO X. Mechanical behavior study of six-bar press[J]. Machine Design & Research, 2013, 29 (4): 143-146.

[6]LU X J, ZHU S H, HE G J, et al. Kinematic analysis of multi-link high-speed presses[J]. China Mechanical Engineering, 2011(11): 1297-1301.

[7]HE Y P, Zhao S D, Zou J, et al. Research on hybrid input mechanical press driven by two motors[J]. International Journal of Mining Science and Technology, 2006, 16(1): 57-60.

[8]LU X J, KE Z M, ZHU S H, et al. Research on slider motion curves of multi-link high-speed press based on virtual prototype technology[J]. Forging & Stamping Technology, 2010, 35(4): 90-94.

(下转第 116 页)

[16]康小宁,屈亚军,焦在滨,等. 基于最小二乘矩阵束算法的工频分量提取方法[J]. 电力系统自动化,2014,38(21):66-70.
KANG Xiaoning,QU Yajun,JIAO Zaibin,et al. Power-frequency phasor extraction based on least-square matrix pencil algorithm[J]. Automation of Electric Power Systems,2014,38(21):66-70.
[17]索南加乐,王斌,宋国兵,等. 电力系统快速相量提取算法的性能探究[J]. 电力科学与技术学报,2013,28(1):25-30.
SUONAN Jiale,WANG Bin,SONG Guobing,et al. Performance study of fast phasor calculating method for power systems [J]. Journal of Electric Power Science and Technology,2013,28(1):25-30.
[18]王晨清,宋国兵,汤海雁,等. 距离保护在风电接入系统中的适应性分析[J]. 电力系统自动化,2015,39(22):10-15.
WANG Chenqing,SONG Guobing,TANG Haiyan,et al. Adaptability analysis of distance protection in power systems with wind farms [J]. Automation of Electric Power Systems,2015,39(22):10-15.

(责任编辑:吕海亮)

(上接第 90 页)

[9]BALASUBRAMANYAM C,SHETTY A B,SPANDANA K R,et al. Analysis and optimization of an 8 bar mechanism[J]. International Journal of Machine Learning and Cybernetics,2015,6(4):655-666.
[10]KIRECCI A,DULGER L C. A study on a hybrid actuator[J]. Mechanism & Machine Theory,2000,35(8):1141-1149.
[11]DU R,GUO W Z. The Design of a new metal forming press with controllable mechanism[J]. Journal of Mechanical Design,2003,125(3):582-592.
[12]GUO W Z,HE K,YEUNG K,et al. A new type of controllable mechanical press:Motion control and experiment validation [J]. Journal of Manufacturing Science & Engineering,2005,127(4):731-742.
[13]LI H,ZHANG C,MENG C. Hybrid-driven nine-bar press for precision drawing[J]. Chinese Journal of Mechanical Engineering,2004,17(S):197-200.
[14]ZHOU Y. Type synthesis and optimization of main driving mechanism for servo-punch press[J]. Journal of Mechanical Engineering,2015,51(11):1-7.

(责任编辑:李 磊)

(上接第 96 页)

[13]孙正龙,王雨薇. 浅谈互联电网低频振荡的分析与控制方法[J]. 黑龙江科技信息,2015(36):180-181.
SUN Zhenglong,WANG Yuwei. Analysis and control of low frequency oscillation in interconnected power system[J]. Heilongjiang Science and Technology Information,2015(36):180-181.
[14]宋鹏程,甄宏宁,王震泉,等. UPFC 附加阻尼控制器设计研究[J]. 江苏电机工程,2015,34(6):10-13.
SONG Pengcheng,ZHEN Hongning,WANG Zhenquan,et al. Parameters tuning for UPFC auxiliary damping controller design of additional damping controller[J]. Jiangsu Electrical Engineering,2015,34(6):10-13.
[15]KHODABAKHSHIAN A,ESMAILI M R,BORNAPOUR M. Optimal coordinated design of UPFC and PSS for improving power system performance by using multi-objective water cycle algorithm[J]. International Journal of Electrical Power and Energy Systems,2016,83:124-133.

(责任编辑:李 磊)